CONF-800432--1

LA-UR -80-922

**TITLE:** CHARACTERIZATION OF MULTIPLE-PHOTON ABSORPTION AND DISSOCIATION OF POLYATOMIC MOLECULES

**MASTER**

**AUTHOR(S):** O'Dean P. Judd

**SUBMITTED TO:** Talk to be presented at the Second International Conference on Multiphoton Processes in Budapest, Hungary April 14-18, 1980



los alamos
scientific laboratory
of the University of California
LOS ALAMOS, NEW MEXICO 87545

An Affirmative Action/Equal Opportunity Employer

DISTRIBUTION OF THIS DOCUMENT IS UNLIMITED

Form No. 836
St. No. 2629
1-79

UNITED STATES
ENERGY RESEARCH AND
DEVELOPMENT ADMINISTRATION
CONTRACT W-7405-ENG-36

# CHARACTERIZATION OF MULTIPLE-PHOTON ABSORPTION AND DISSOCIATION OF POLYATOMIC MOLECULES*

O. P. Judd
University of California
Los Alamos Scientific Laboratory
Los Alamos, NM

Talk to be presented at the
Second International Conference
on Multiphoton Processes
Budapest, Hungary
April 14-18, 1980

*Work performed under the auspices of the U.S. Department of Energy.

## ABSTRACT

A quantitative comparison of multiple-photon absorption (MPA) and dissociation (MPD) has been performed for experiments with a number of different polyatomic molecules. Appropriate normalization techniques for the absorption and dissociation parameters are formulated to account for the different conditions of the experiment and the molecular parameters. This procedure in a first approximation, accounts for the effects of independent variables such as gas pressure, optical bandwidth, optical pulse duration, excitation frequency, spectral width of the optical absorption band, absorption strength of the transition, bond strength, and the density of states in the molecule. The theoretical description of the dynamics of the absorbing ground state is considered and used to provide the rationale for the normalization procedure.

The results of this analysis indicate that the functional dependence of the number of photons absorbed per molecule with fluence is qualitatively the same for the most molecules. Similarly, the probability for dissociation of most molecules can be related to the density of vibrational states, the bond strength, the number of photons absorbed per molecule, and the width of the absorbing transition.

The functional relationships derived for MPA and MPD can be related to several theoretical aspects of the optical interaction process. In particular, the implications for the basic absorption mechanisms and the distribution of vibrational energy in the molecule will be addressed.

## I. INTRODUCTION

In order to gain a better understanding of the fundamental mechanisms involved in the multiple-photon excitation (MPE) of polyatomic molecules, we have performed a semiquantitative comparison study of multiple-photon absorption (MPA) and dissociation (MPD) experiments that have been reported in the literature. From this study, we obtain the general functional dependence for MPA and MPD on laser fluence, and the general dependence of these processes on the properties of the molecule, the radiation field, and the thermodynamic conditions of the gas.

In order to compare the MPE experiments for different molecules, it is necessary to specify a quantitative measure of the strength of the interaction between the molecule and the optical field and the related molecules response to this interaction. This necessitates the identification of the important independent variables involved in the interaction and an appropriate normalization for these variables. An initial study of this type for MPA has been described previously.[1] We will briefly review the methodology and results of this work and discuss more recent developments involving $NH_3$ in Sec. II. A similar study has been performed for MPD[2] and will be discussed in Sec. III. The implications of these results for basic mechanism related to MPE is also considered. Measurements that relate to the vibrational-energy distribution for excited $SF_6$ are discussed in Sec. IV.

## II. MULTIPLE-PHOTON ABSORPTION

The measurements of absorption of infrared radiation in polyatomic molecules are conventionally described in terms of the absorption cross section $\sigma(\Phi)$ or the number of photons absorbed per molecule $\eta(\Phi)$ as a function of the optical fluence $\Phi$ or intensity $\phi$. In general, $\eta(\Phi) \neq \sigma(\Phi)\Phi$.

At sufficiently low fluence, this interaction can be described in terms of an effective two-level system. As the fluence increases from zero, the cross section is a constant $\sigma_o$ up to a fluence value $\Phi_s$, at which point $\sigma(\Phi)$ decreases as $\Phi^{-\nu}$. For a strict two-level system, $\nu = 1$. Physically, at this fluence, a significant fraction of the population of the ground state of the transition is transferred to the upper level. For MPE, population is removed from the upper level of the transition by optical absorption, so that this description will not be valid. For example in $SF_6$, experiments indicate that for $\Phi_s < \Phi < \Phi_D$, $\nu = 1/3$,[3] where $\Phi_D$ is the fluence for dissociation of 1% of the molecules. Nevertheless, the two-level approximation can provide a guide for normalization of the dependent and independent variables involved in the interaction. For MPA, we consider the same normalized variables but in a more general functional form than that for the two-level system. Although the presence of rotational levels and strong coupling to other vibrational levels complicates the concept of an isolated two-level interaction, these effects do not qualitatively change the above description and they can be included in a straightforward manner in the formulation of a generalized two-level model.

The coupled two-level absorber model described in Ref. 1 contains the following features. A finite bandwidth radiation field interacts with one or several rotational states of a vibrational level of a molecule to promote transitions to an upper vibrational state. We consider this interaction in a rate equation approximation. This interaction results from the direct spectral overlap of the radiation field and the absorbing transition of the molecule. Other rotational states that are not coupled directly to the radiation field constitute a set of reservoir states that may be indirectly coupled to the interacting rotational levels through collisions. Also included in the reservoir states are other vibrational levels that are

coupled to the interacting states either by collisional or collisionless intramodal V-V' transfer processes.

Reference 1 gives an approximate solution to the differential equations that describe optical and collisional transitions among the four levels of the model (two absorber levels and two reservoir levels). The results of this analysis gives

$$\frac{\eta(\Phi)}{\langle f \rangle} = 1 - \exp\left(-\frac{\sigma_o \Phi}{\langle f \rangle}\right) \tag{1}$$

for the relationship between the average number of photons absorbed per molecule, $\eta(\Phi)$, and the three variables $\Phi$ (fluence), $\sigma_o$ (small signal absorption cross section), and $\langle f \rangle$ (the effective fraction of the population for a given vibrational transition that is coupled to the radiation field). In the strong fluence limit the quantity $\langle f \rangle$ is

$$\langle f \rangle = d\, f_i \left[1 - \exp\left(-\frac{f_r}{1-f_r}\,\frac{\tau_p}{\tau}\right)\right] \tag{2}$$

where $f_i$ fraction of molecules in the absorbing (usually ground) vibrational level and $f_r$ is the fraction of the $f_i$ molecules in the initial distribution that interact directly with the radiation field. The value of $f_r$ is determined by the spectral overlap of radiation field and the absorption spectrum of the molecule. The quantity $d_i$ is

$$d = \frac{\beta}{1+\beta} \tag{3}$$

where $\beta$ is the ratio of degeneracies of the upper and lower vibration levels; $\tau_p$ is the optical pulse length; and $\tau$ is the absorber level/reservoir

level equilibration time (usually taken as rotational relaxation time). If the pressure is sufficiently high, the value oi <f> exceeds d $f_i f_r$ due to collisional coupling of the absorber and reservoir levels. A more general form for <f> is given in Ref. 1.

Cast in this general form, the optical interaction in a coupled two-level system can be described in terms of two parameters, a fluence parameter $\sigma_0\Phi/\langle f\rangle$ and the effective fraction of states that interact with the radiation field <f>. All effects due to collisions ($\tau$), intramolecular V-V' coupling ($\tau$), laser pulse duration ($\tau_p$), gas temperature ($f_i$, $f_r$, $\tau$), pressure ($\tau$), and laser spectral bandwidth ($f_r$) can be regarded in first approximation as affecting the effective fraction of absorber molecules <f> that can be coupled to the radiation field.

For multiple-photon excitation, we consider as an ansatz the interaction in the general functional form.

$$\frac{\eta(\Phi)}{\langle f\rangle} = G\left(\frac{\sigma_0\Phi}{\langle f\rangle}\right) \tag{4}$$

Data for $SF_6$, for example, indicate that $G(x) \propto x^{2/3}$ for $x \gg 1$. For $x \ll 1$, the two-level result is obtained for which $G(x) = 1 - \exp(-x)$. As pointed out in Ref. 1, a normalization of this type is only valid at frequencies near the center frequency $\nu_0$ of the molecular absorption feature for which $\sigma_0 \gtrsim 0.1\,\sigma_0(\nu_0)$.

A plot of MPA data for several molecules is shown in Fig. 1. This particular form of the data summary indicates the general nature of the MPE process and the fluence range over which these processes are observed. The extent of the range for MPA is only apparent, however, because the fluence variable alone does not constitute a good measure of the interaction of the radiation field with the molecule.

A considerable simplification results if these absorption data are replotted in terms of $\sigma_o\Phi$. The results are shown in Fig. (2). With the exception of the triatomic molecules, the fluence behavior of the different molecules can be classified into two types: (1) one in which a deviation from linear absorption begins to occur; and (2) one in which $\eta \propto \Phi^{\gamma}$ where $\gamma \cong 2/3$. The general functional behavior of each molecule is consistent with Eq. (3) depending on whether $\sigma_o\Phi/\langle f\rangle$ is greater than or less than unity. The factor that has not been taken into account for the different molecules in Fig. (2) is $\langle f\rangle$. If $\langle f\rangle$ could be calculated for each molecule and the absorption data could be replotted in the normalized form of Eq. (3), the curves in Fig (2) would be expected to merge into a single curve. In practice, $\langle f\rangle$ is difficult to calculate from first principles. Since $\langle f\rangle$ is a divisor in both the dependent and independent variables in Eq. (3), we can obtain the ratio of $\langle f\rangle$ for two molecules by simply shifting each plot of $\eta(\Phi)$ vs. $\sigma_o\Phi$ in Fig. (2) along the linear absorption line until the curves merge. This procedure is tantamount to multiplication or division of the ordinate and abscissa of a given logarithmic graph by a constant. For convenience, we take the curve for $S_2F_{10}$ as a reference and shift the remaining curves accordingly. The results are shown in Fig. 3. The values of the ordinate and abscissa are nearly absolute[1]. As expected on physical grounds, all of the data can be fitted to a single curve for $\sigma_o\Phi/\langle f\rangle \leq 1$. It is surprising, however, that nearly the same functional dependence is obtained for all molecules at high fluence. With the exception of $SF_6$ and the triatomics, all molecules dissociate at some point on the curve. For the large polyatomic molecules, $CH_3COCF_3$, $S_2F_{10}$, and $SF_5NF_2$, significant dissociation occurs at $\sigma_o\Phi/\langle f\rangle \leq 1$; i.e., in the range of "linear absorption." For values of $\sigma_o\Phi/\langle f\rangle \leq 1$, it appears that most molecules, when

excited at a frequency near the peak of the absorbing transition, absorb energy with a fluence dependence of $\Phi^{2/3}$.

The functional behavior of $\eta(\Phi)$ appears to be similar for most large polyatomic molecules. The triatomic molecules appear to behave as a classical two-level system and do not exhibit MPE behavior in the fluence range indicated. It is of interest to consider a four-atom molecule to evaluate its MPE behavior. Several studies of MPD of $NH_3$ have been reported in the literature. Measurements of MPA have also been recently reported[4] over a pressure range of $5 \leq P < 244$ torr and a fluence range of $0.04 \leq \Phi \leq 0.7$ J/cm$^2$. The excitation frequency of 1076.0 cm$^{-1}$ [R(16) $CO_2$ laser line] coincides most nearly with the aR(6,0) transitions of the $\nu_2$ vibrational mode in $NH_3$. The off resonance detuning from the aR(6,0) is 0.021 cm$^{-1}$ and from the aR(6,1) is 0.12 cm$^{-1}$. The small signal absorption consequently results from two overlapped wings of these two pressure-broadened lines and is reflected in the pressure dependence of $\sigma_0$. By plotting the absorption in terms of $\eta(\sigma_0\Phi)$, this particular source of the pressure dependence should be removed in a zero-order approximation. The results are shown in Fig. 4. As is apparent, most of the absorption data can be fit to a single curve over the complete range of fluence and pressure used in the measurement.

Several conclusions follow from this result. Apparently most of the pressure dependence of the optical absorption in $NH_3$ results from the spectral overlap behavior manifest in $\sigma_0$. If the collision dynamics of the MPE process were affected by the pressure, the simple normalization of $\sigma_0\Phi$ would not be expected to result in a single curve for a factor-of-40 change in pressure. A comparison of the curve in Fig. 4 with the data for MPA in other polyatomic molecules (Fig. 1) indicates good qualitative agreement in

terms of the functional dependence. Although there is some scatter in the data at high fluence, the $NH_3$ fluence behavior is not inconsistent with the 2/3 slope that is observed for MPA in other polyatomic molecules. The additional parameter that characterizes this interaction is the effective fraction of the molecular population that interacts with the radiation field $\langle f \rangle$. A comparison of $NH_3$ with other polyatomic molecules indicates at $\langle f \rangle \tilde{\sim} 1$, which means physically that all of the population of the vibrational ground state is interacting with the optical field. This is also consistent with the fact that $\eta$ is independent of pressure.

At low fluence, the fraction of molecular population that is directly accessed by the optical field $f_r$ is determined primarily by the Boltzmann thermal population of the $J = 6$, $k = 0$, 1 rotational levels and the Lorentzian lineshape factors. This fraction is much smaller than unity. During the optical pulse $\tau_p$, collision-induced rotational equilibration will couple these levels to all other rotational levels in the manifold. In order that $\langle f \rangle \tilde{\sim} 1$ and $\eta$ be independent of pressure, the rotational equilibration time, $\tau_r$, must satisfy the condition that $f_r \tau_p / \tau_r \gg 1$. (cf. Eq.2) Measurements of the optical dephasing time and the population decay time for $NH_3$ have been reported for both the ground and excited vibrational states. These measurements indicate that $\tau_r$ may be anomalously short and in the range of 0.05-0.2 of the gas-kinetic value (125 ns-torr). Using a value of 0.1, $\tau_r \tilde{\sim} 2$ ns at 5-torr pressure. If $\tau_p \tilde{\sim} 200$ ns, $f_r \gtrsim 0.01$ to satisfy the required criteria.

The functional dependence of the fluence-dependent absorption of $NH_3$ is characteristic of MPA in a large number of polyatomic molecules. This is somewhat surprising from the viewpoint of the current theoretical mechanisms proposed for MPE. In $NH_3$ the density of states is low and the

anharmonicities are large; consequently, a compensation of the anharmonicity by power broadening would only occur at high optical intensities. Because of the specific excitation frequency selected, multistep resonances such as the P-Q-R rotational compensation should also be unimportant. The invariance of the functional dependence of the MPA over such a large pressure range is also of interest. We will return to these points later.

The fact that higher fluences are required for MPE (and probably MPD) in $NH_3$ than in other polyatomic molecules may be due to the weak absorbing feature being accessed by the optical field ($\sigma_o \approx 5 \times 10^{-20}$ $cm^2$) rather than any particular characteristic of the molecule. This follows directly from the data shown in Fig. 4.

The coupled two-level model and the general functional form of the MPA measurements shown in Fig. 3 leads to a number of implications that can be evaluated directly. In particular, it is of interest to explore the functional relationships of gas pressure P, bandwidth of the optical source $\Delta$, temporal pulse shape $\tau_p$, and the dependence on optical flux. In order to gain physical insight into these processes, we consider the effect of rotational relaxation in the optical absorption process. In the fluence range that $\sigma_o\Phi \cdot \tau_p \ll 1$, the trends in Fig. 3 indicate that $\eta(\Phi)$ can be written in the functional form

$$\eta(\Phi) \propto \tau_p^{1/3} \, (\sigma_o\Phi)^{2/3} \quad . \tag{5}$$

The value of $\sigma_o$ is determined primarily by the properties of the particular molecule. The collisional effects and most other experimental parameters are manifest in $\tau_p$. This proportionality provides the dominant functional

relationship for the dependence of $\eta(\Phi)$ on $\tau_p$, P, and $\Delta$. Let $\tau$ be the rotational equilibration time; $\tau \propto P^{-1}$. If the gas pressure is sufficiently low that for $\tau_p/\tau \ll 1$, the limiting form of Eq. (2) gives the result that $\eta(\Phi) \propto P^{1/3}\Phi^{2/3}$. A comparison with pressure dependent absorption data for $SF_6$ using xenon as a buffer gas is shown in Fig. 5. The values of $\tau$, and $f_r$ can be evaluated directly. Over the pressure range $0.1 < P < 10$ torr, the $P^{1/3}$ pressure dependence of $\eta$ is clearly evident. The solid curves in the figure are the calculated values of $\eta(\Phi)$ from eqs. 2 and 5. The ordinate of the curves have been adjusted at one point to agree with the absolute value of the measured absorption. A good fit to the experimental data is observed over the complete range of fluence and pressure.

The results of the comparison of experimental data for several polyatomic molecules in terms of the normalized variables indicates that MPA for almost all polyatomic molecules can be described by a single function of fluence. It appears from this comparison that multiple-photon absorption in polyatomic molecules is a general phenomena that is qualitatively the same for all molecules; quantitative differences can be related to differences in $\sigma_0$ and $f_r$. Since $\sigma_0$ and $f_r$ predominantly characterize the initial interaction dynamics of the radiation field with the lower level of the molecular transition, it appears that the absorption dynamics is dominated by this process and not by any specific MPE process. Consequently it appears that absorption measurements are not a sensitive test of MPE theory.

That fact that $\eta \propto \Phi^{2/3}$ may be characteristic of the MPE process. This result is consistent with and a direct consequence of the anharmonic model for MPE[5]. The fact that $NH_3$ follows a similar dependence may or may not be fortuitous. Several theoretical models involving collisional relaxation and/or thermal heating of the rotational levels can also quantitatively account for this behavior in the range of the higher pressures.

Consequently the $\Phi^{2/3}$ fluence dependence is not unique to a MPE process. At the present time, it appears that the fluence dependent absorption is generically the same for most polyatomic molecules and that the 2/3 power dependence may be characteristic of the MPE process.

III. Multiple-photon Dissociation

A similar study can be performed for dissociation experiments as was done for absorption. In this case, however, the results should be more sensitive to the MPE dynamics of the interaction. In addition to the parameters $\sigma_o$ and $\langle f \rangle$, the probability for dissociation should also depend on the density of vibrational states $N(E_v)$, the bond strength $E_A$, the width of the absorption band $\nu_{1/2}$, and the frequency offset from the band center $\Delta\nu$. It may also depend on the molecular symmetry, the lowest frequency vibrational mode in the molecule, and internal rotations. The value of $\nu_{1/2}$ and $f_r$ used in the absorption analysis are related in that $\nu_{1/2} \propto f_r^{-1}$. The effect of multiphoton resonances is related to the irradiation frequency and consequently $\Delta\nu$.

As a quantitative measure of dissociation, we have evaluated the laser fluence ($\Phi_{1\%}$) necessary to give a reaction probability of 1% for a number of molecules. In a subset of these experiments, it was also possible to determine the value of $\eta_{1\%}$. Since the density of vibrational states is an important parameter in theories of MPE as well as theories of unimolecular reactions, we consider a plot of $\Phi_{1\%}$ as a function of the density of vibrational states at an energy of 10'00 $cm^{-1}$. This value represents about 11 $CO_2$ laser quanta and is about the average excitation necessary to give a 1% reaction probability for a thermal vibrational energy distribution in a sample of molecules with a moderate activation energy (60 kcal/mol). From the absorption experiments we observed that the normalized fluence was

expressed in the form $\sigma_o\Phi_{1\%}/\langle f\rangle$. Since $\eta_{1\%}$ and $\sigma_o\Phi_{1\%}/\langle f\rangle$ are directly related (Fig. 3), we consider a dissociation parameter $\sigma_o\Phi_{1\%}\ \nu_{1/2}\ /E_a$ which is the measure of the energy absorbed in the molecule that gives 1% dissociation probability, compared to the activation energy of the molecule. A plot of this parameter as a function of N(10500) is shown in Fig. 6. The vertical bars show the range of $\Phi_{1\%}$ from different data sources or from different frequencies within the absorption band. In terms of this parameter, the dissociation of most molecules is strongly correlated with the vibrational state density. As indicated in the plot, the value of $\Phi_{1\%}$ decreases with $N(E_v)$, a trend already well known from the literature. Even after correction for the small-signal cross section, the band width, and the activation energy, the larger molecules (higher vibrational-state density) still tend to react more easily.

It is also of interest to determine the dependence of the dissociation probability on the frequency within the molecular absorption band and the distribution of vibrational energy within the molecule. For this purpose we plot in Fig. 7 the measured amount of absorbed laser energy necessary to give 1% reaction as a fraction of the activation energy, $\eta_{1\%}/E_a$, versus $\Delta\nu/\nu_{1/2}$. The dashed line is the value of $\eta_{1\%}/E_a$ for a thermal reaction. This plot shows to some extent how the absorbed laser energy is distributed over the available vibrational states. For the points below the dashed line the distribution over vibrational states is broader than a thermal distribution. That is, the amount of energy absorbed is less than a thermal distribution would give when 1% of the sample molecules have sufficient energy to react. The broad distribution could be due to an enhanced absorption cross section at high levels of vibrational excitation, to the fact that only a fraction of the molecules in the sample interacting with the

laser field, or to the tendency of the absorbed radiant energy to remain in the absorbing mode. A narrow distribution, which would give points above the dashed line, could result from diminished absorption cross section at high levels of excitation. Points above the dashed line could also result from a non-negigible recombination rate. The clustering of most of the points around the dashed line indicates that most of the vertical scatter in Fig. 7 is due to differences in how much laser energy is actually absorbed, and that differences in how that absorbed energy is distributed are smaller, but not negligible.

Where detailed data are available, a comparison can be performed between the dissociation produced by optical excitation and by thermal excitation of the vibrational levels in the molecule. We find that the experimental reaction probabilities generally have shapes that are similar to the thermal curves, but in most cases the experimental curves deviate significantly from the thermal curves. The frequency of the exciting radiation is an important parameter. The reaction probability curves tend to be close to thermal for frequencies near the band center (for $S_2F_{10}$, $CF_3COCF_3$, and $SF_5NF_2$); however, for frequencies in the high- and low-frequency extremes of the bands, the absorbed laser energy produces reaction much more efficiently. It may be the case that in the extremes of the bands, the laser interacts with a smaller fraction of the molecules.

The dissociation correlations discussed above are not necessarily unique. From the viewpoint of molecular excitation and deexcitation, the interaction dynamics may also depend on the lowest frequency vibrational mode in the molecule. A plot of $\eta_{1/2}/\tau$ (as determined from Fig. 3) as a function of the energy of the lowest frequency vibrational mode $E_V$ (min) is shown in Fig. 8. Again the functional correlation is satisfactory. The

density of vibrational states is only indirectly related to $E_V$ (min) and consequently Figs. 6 and 8 are conceptually different relations.

## III. Vibration energy Distribution

From the study of dissociation of a number of polyatomic molecules, indirect evidence suggests that the vibrational energy distribution produced by optical excitation is non-thermal. Recent pulse-probe measurements have been performed that confirm this conclusion for $SF_6$.[6] Shown in Fig. 9 is the spectral absorption cross section measured by a cw probe laser at several delay times after excitation by a strong pulsed laser operating at a frequency of 947.7 $cm^{-1}$. At time zero, the figure shows the total spectroscopic absorption cross section for $^{32}SF_6$, $^{33}SF_6$ and $^{34}SF_6$ at a temperature of 145 K. At 5 μs, the molecule has absorbed 2.6 photons ($\Phi$ = 0.54 $J/cm^2$) from the optical field and the laser pulse is terminated. The strong red shifts in the absorption spectrum are indicative of high levels of vibrational excitation in the molecule. The curves at subsequent times indicate the relaxation of the vibrational energy distribution. A curve showing the spectral absorption produced by a thermal vibrational distribution (500 K) is also shown for purposes of comparison. The temperature of 500 K is the thermal equivalent energy of 2.6 $CO_2$ laser photons. As is evident from the figure, the laser produced distribution is strongly non-thermal and exhibits a long high energy tail.

References

(1) O. P. Judd, J. Chem. Phys. 71, 4515 (1979).

(2) J. L. Lyman, G. P. Quigley, and O. P. Judd, "Single-infrared Frequency Studies of Multiple-photon excitation and Dissociation of Polyatomic Molecules" in Multiple-Photon Excitation and Dissociation of Polyatomic Molecules, C. D. Cantrell, ed., Springer-Verlag (to be published).

(3) J. L. Lyman and K. M. Leary, J. Chem. Phys. 68, 1858 (1978).

(4) V. Starov, C. Steel and R. G. Harrison. J. Chem. Phys. 71, 3304 (1979).

(5) See Ref. 1 and the references therein.

(6) J. L. Lyman, L. J. Radziemski and A. C. Nilsson (submitted to J. Quant. Electron.)

Figure Captions

(1) Fluence dependent absorption data for a number of polyatomic molecules.

(2) Fluence dependent absorption data as a function of the normalized fluence $\sigma_0\Phi$.

(3) Plot of multiple-photon absorption data in terms of the normalized variables $\eta(\Phi/\langle f\rangle$ and $\sigma_0\Phi/\langle f\rangle$.

(4) Functional dependence of $\eta(\Phi)$ with pressure, with fluence as a parameter. The points are experimental data. The solid curves are the calculated dependence; the ordinate have been normalized at one data point.

(5) Plot of $\eta(\Phi)$ as a function of $\sigma_0\Phi$ for $NH_3$.

(6) Plot of the normalized dissociation parameter $\Phi_{1\%}\sigma_0\nu_{1/2}/E_a$ versus the density of vibrational states at 10500 $cm^{-1}$.

(7) Normalized dissociation energy $\eta_{1\%}/E_a$ versus $\Delta\nu/\nu_{1/2}$.

(8) Normalized dissociation energy $\eta_{1\%}/\langle f\rangle$ versus the frequency of the lowest vibrational mode in the molecule.

(9) Spectral absorption cross-section for laser excited $SF_6$ as measured by a cw probe laser at various times in the excitation sequence.

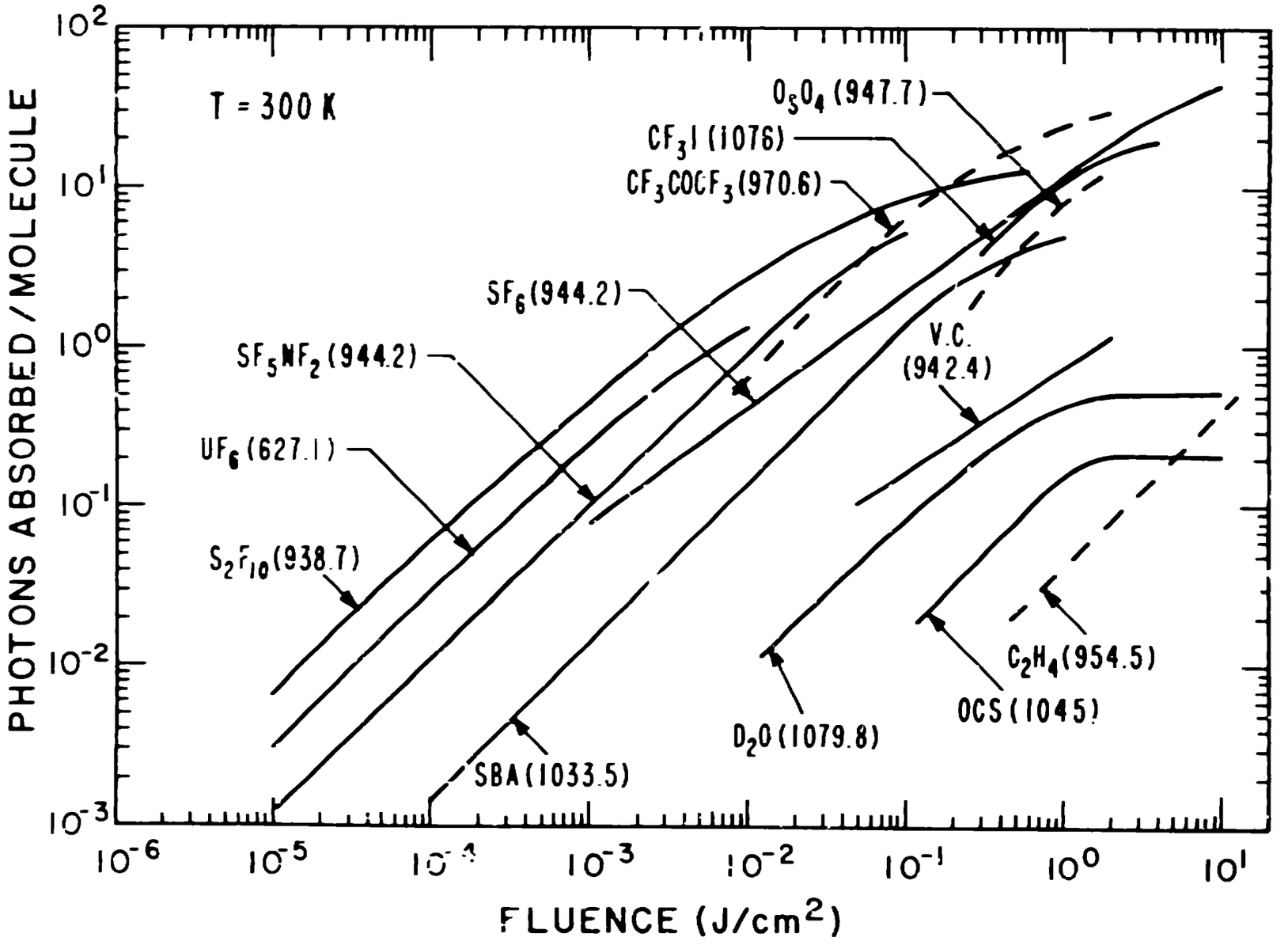
T = 300 K
$O_3O_4$ (947.7)
$CF_3I$ (1076)
$CF_3COCF_3$ (970.6)
$SF_6$ (944.2)
$SF_5NF_2$ (944.2)
V.C. (942.4)
$UF_6$ (627.1)
$S_2F_{10}$ (938.7)
$C_2H_4$ (954.5)
OCS (1045)
$D_2O$ (1079.8)
SBA (1033.5)
PHOTONS ABSORBED / MOLECULE
FLUENCE (J/cm$^2$)
$10^2$
$10^1$
$10^0$
$10^{-1}$
$10^{-2}$
$10^{-3}$
$10^{-6}$
$10^{-5}$
$10^{-4}$
$10^{-3}$
$10^{-2}$
$10^{-1}$
$10^0$
$10^1$

Figure 1

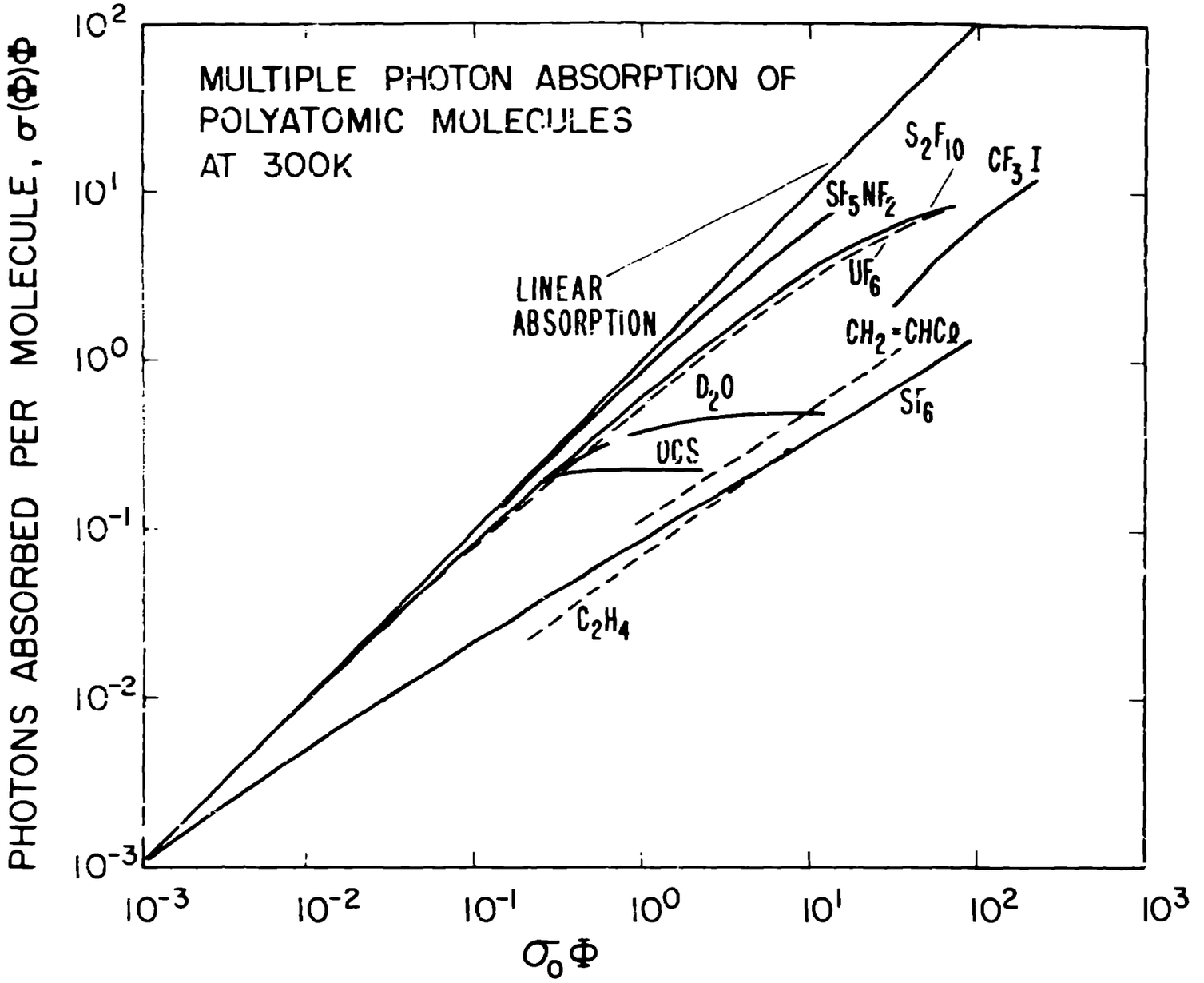
MULTIPLE PHOTON ABSORPTION OF
POLYATOMIC MOLECULES
AT 300K
PHOTONS ABSORBED PER MOLECULE, σ(Φ)Φ
$\sigma_0\Phi$
LINEAR
ABSORPTION
$S_2F_{10}$
$CF_3I$
$SF_5NF_2$
$UF_6$
$CH_2=CHCl$
$D_2O$
$SF_6$
UCS
$C_2H_4$
$10^2$
$10^1$
$10^0$
$10^{-1}$
$10^{-2}$
$10^{-3}$
$10^{-3}$
$10^{-2}$
$10^{-1}$
$10^0$
$10^1$
$10^2$
$10^3$

Figure 2

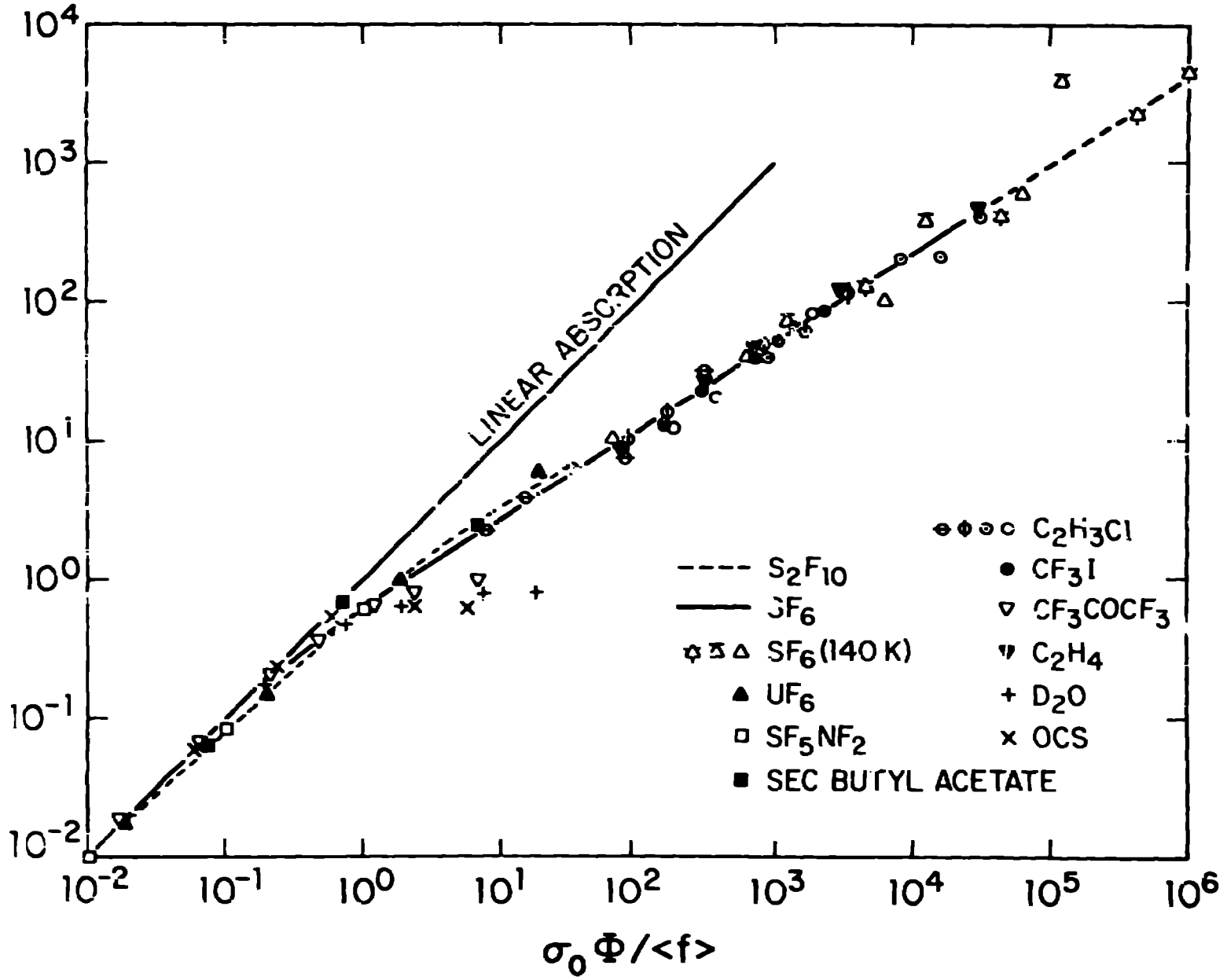
LINEAR ABSORPTION
$S_2F_{10}$
$SF_6$
$SF_6$(140 K)
$UF_6$
$SF_5NF_2$
SEC BUTYL ACETATE
$C_2H_3Cl$
$CF_3I$
$CF_3COCF_3$
$C_2H_4$
$D_2O$
OCS
$\sigma\Phi/\langle f\rangle$
$\sigma_0\Phi/\langle f\rangle$

Figure 5

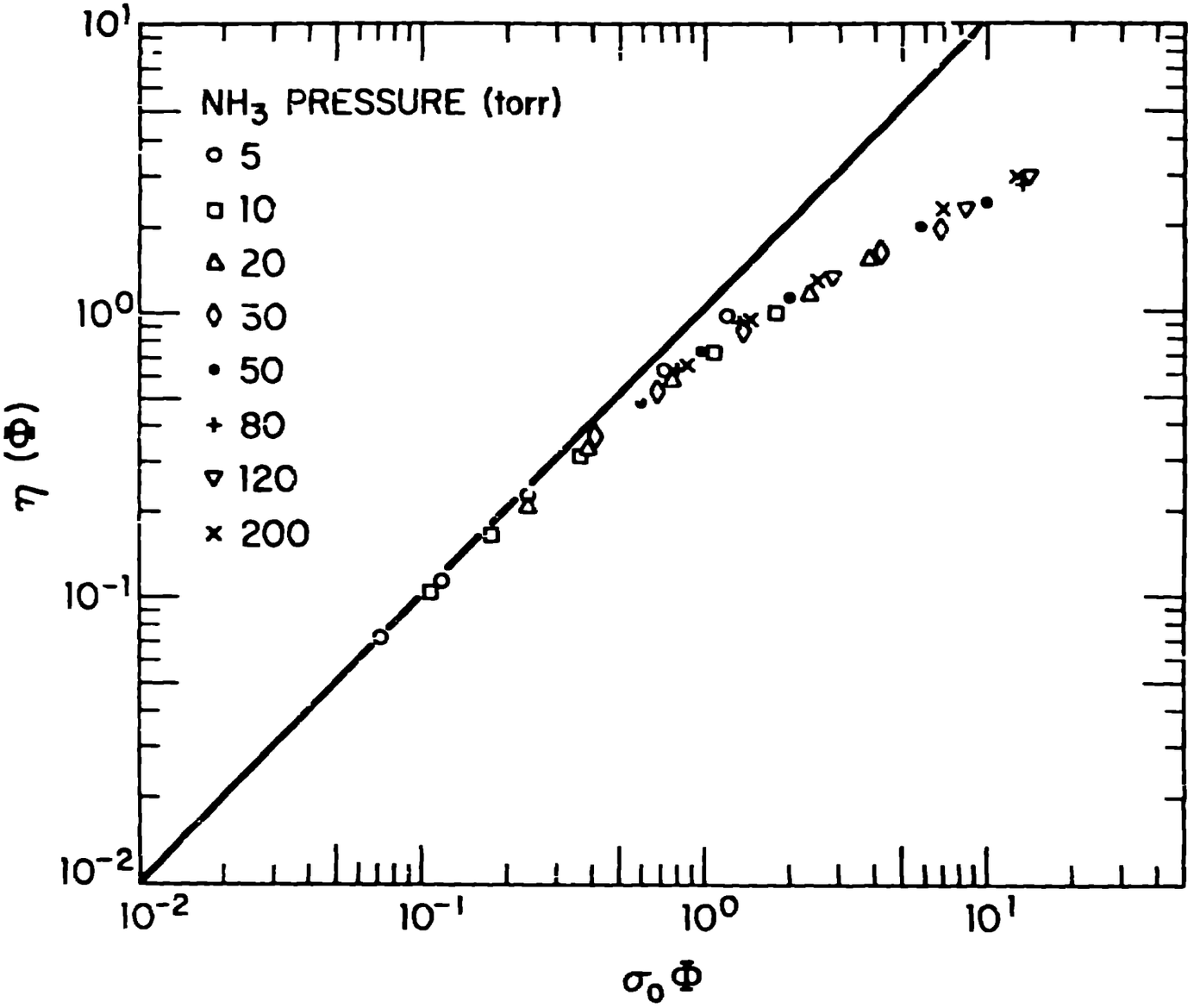


Figure 1

AP-1-VG-4959

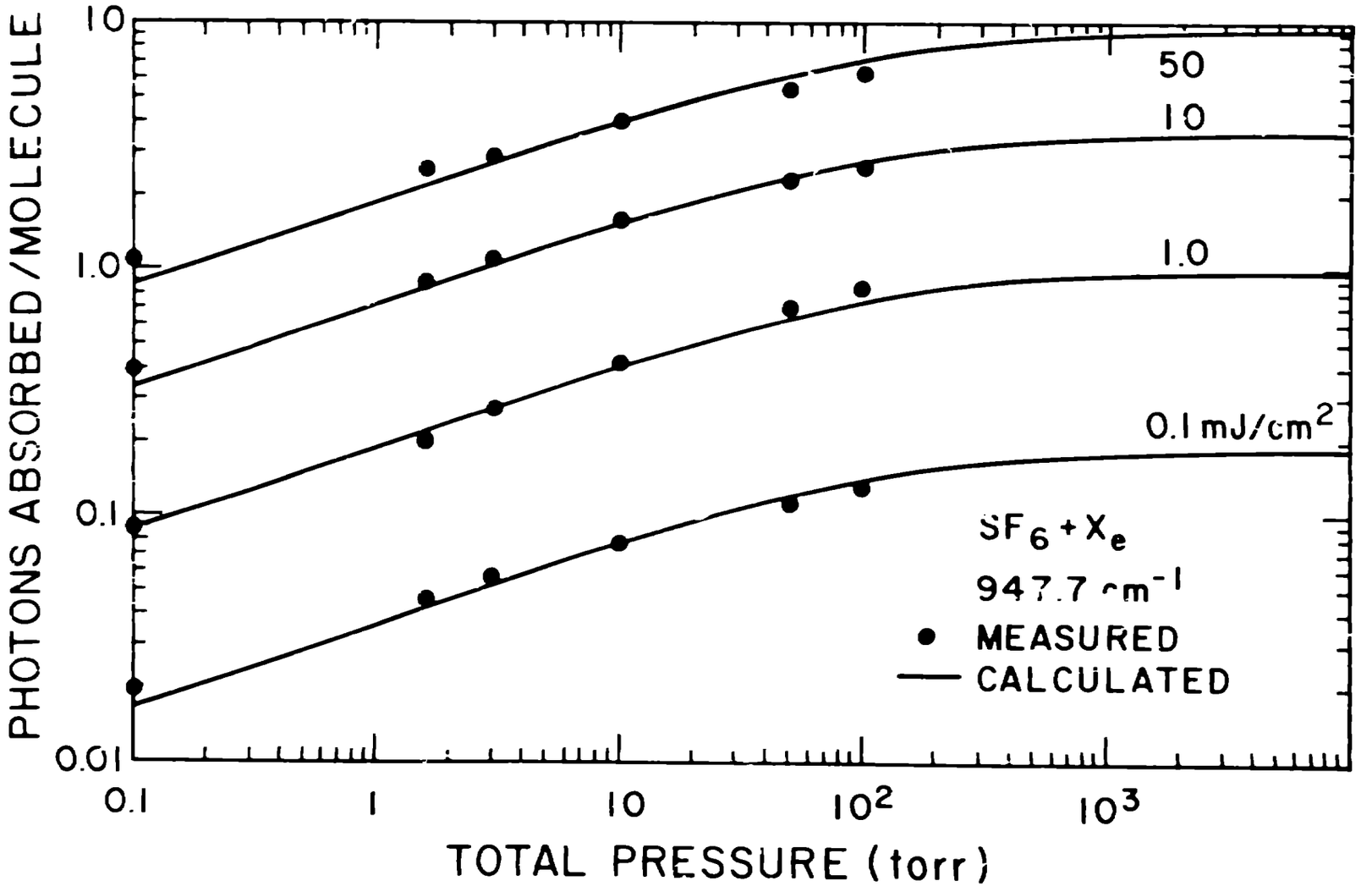
PHOTONS ABSORBED/MOLECULE
10
1.0
0.1
0.01
0.1
1
10
$10^2$
$10^3$
TOTAL PRESSURE (torr)
50
10
1.0
0.1 mJ/cm$^2$
$SF_6 + X_e$
947.7 cm$^{-1}$
MEASURED
CALCULATED

Figure 3

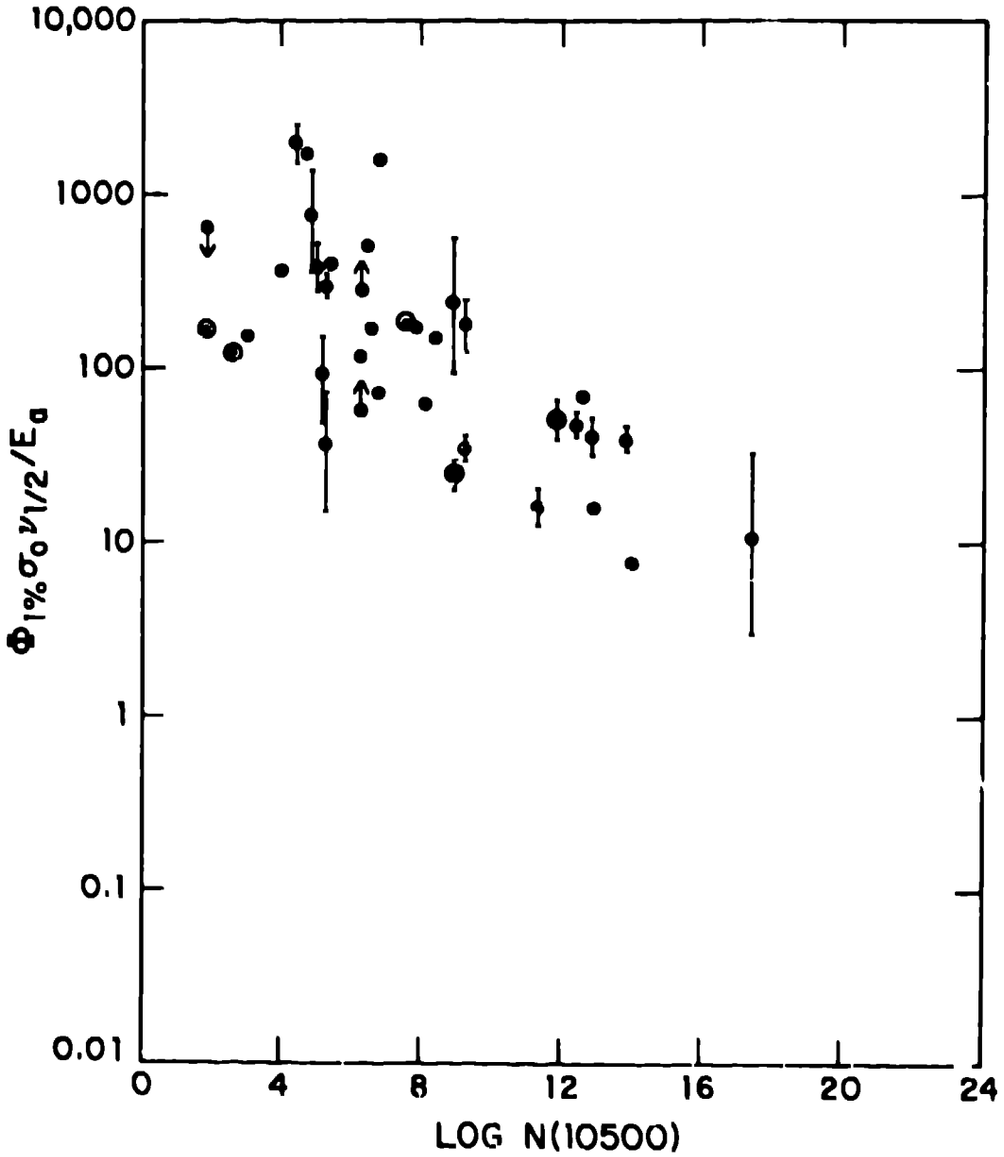
10,000
1000
100
10
1
0.1
0.01
$\Phi_{1\%}\sigma_0\nu_{1/2}/E_a$
0
4
8
12
16
20
24
LOG N(10500)

Figure 6

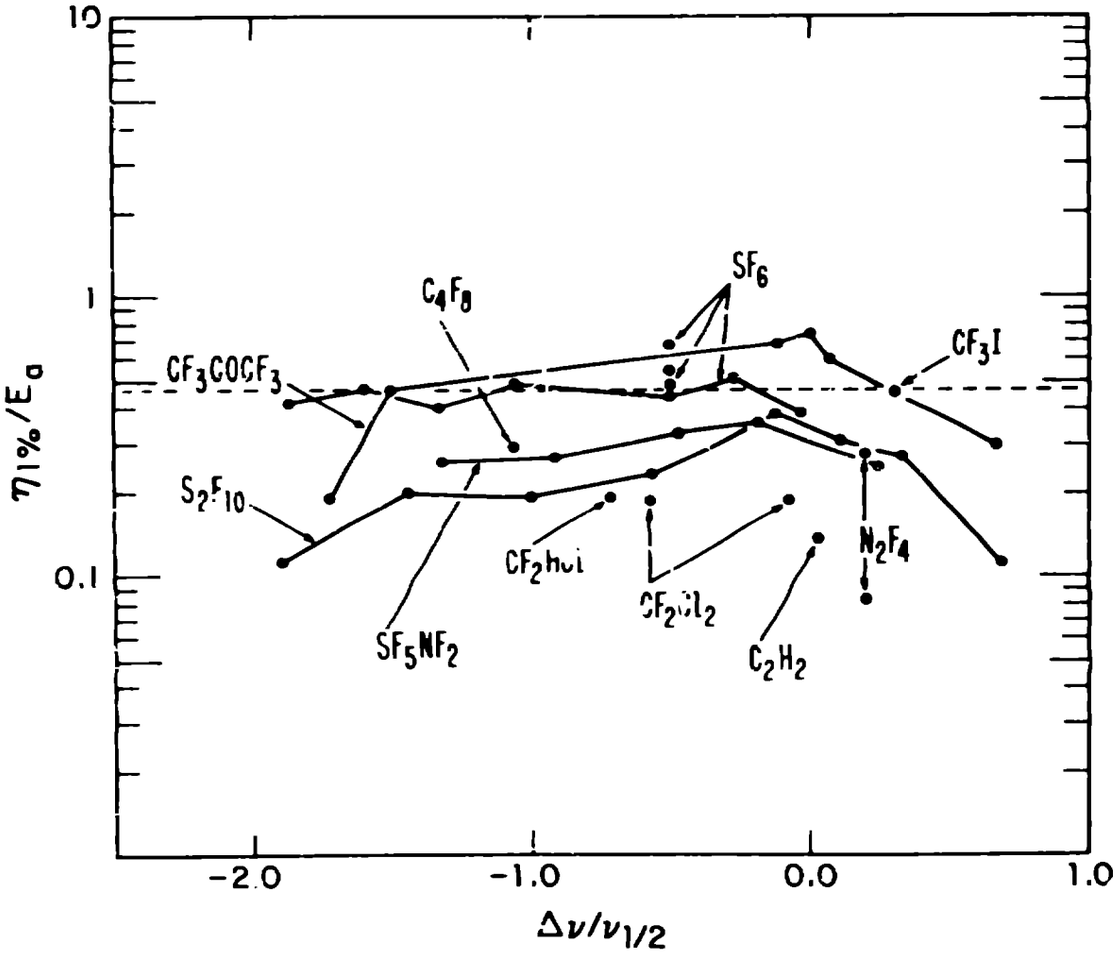
10
1
0.1
$\eta_{1\%}/E_a$
$SF_6$
$C_4F_8$
$CF_3I$
$CF_3COCF_3$
$S_2F_{10}$
$CF_2HCl$
$N_2F_4$
$CF_2Cl_2$
$SF_5NF_2$
$C_2H_2$
-2.0
-1.0
0.0
1.0
$\Delta\nu/\nu_{1/2}$

Figure 7

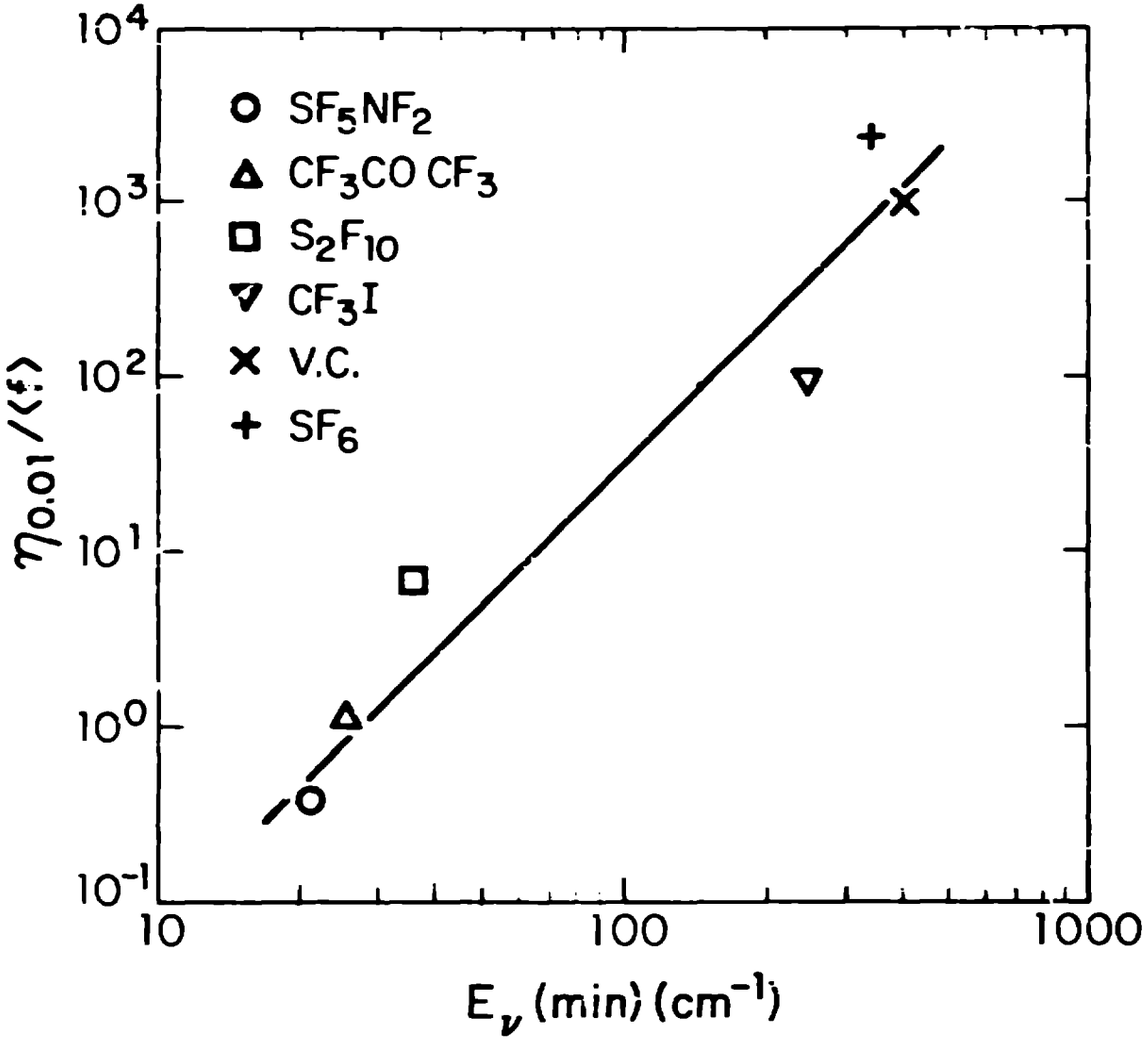


Figure 8



AP-1-VG-4467

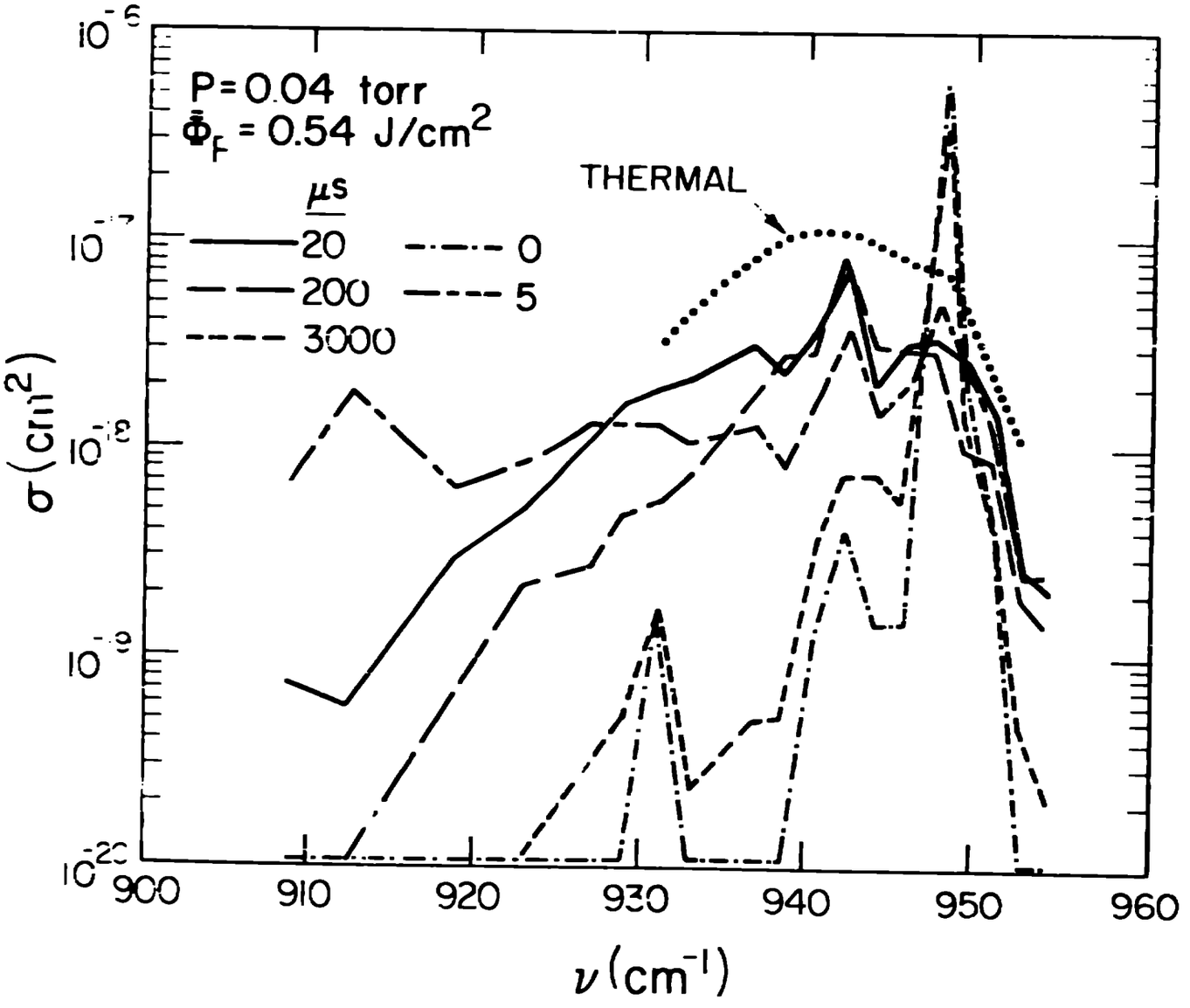
P=0.04 torr
$\Phi_F$ = 0.54 J/cm$^2$
μs
20
200
3000
0
5
THERMAL
$10^{-6}$
$10^{-17}$
$10^{-18}$
$10^{-19}$
$10^{-20}$
σ (cm$^2$)
900
910
920
930
940
950
960
ν (cm$^{-1}$)

Figure 9